*Journal of Sound and Vibration* (2000) **231**(3), 739–751
doi:10.1006/jsvi.1999.2559, available online at http://www.idealibrary.com on IDEAL®

# SIMULATIONS OF GROUND VIBRATION FROM A MOVING HARMONIC LOAD ON A RAILWAY TRACK

C. J. C. JONES, X. SHENG* AND M. PETYT

*Institute of Sound and Vibration Research, University of Southampton, Highfield, Southampton, SO17 1BJ, England*

(*Received in final form* 23 *September* 1999)

A sequence of results is presented from a model of an oscillating load moving on a track on a layered ground. The results allow a visualization of the effect of the relative speeds of the load and the propagation speeds in the ground structure. This is useful in developing the understanding of the interaction of train speed, track structure and ground properties for high-speed trains. The simulation shows the excitation of high amplitudes of vibration in the track, the "bow wave" angle of propagation of vibration in the ground and the transfer of vibrational energy to a higher order mode as the speed of the load exceeds that of the first mode of propagation in the layered ground. 

## 1. INTRODUCTION

As a train runs on a track, vibrations are generated which can propagate through the ground and be detected at nearby properties. For surface propagating vibration generated by mainline trains, vibration is generated with significant components in the frequency range from about 4–80 Hz. Prediction of such phenomena requires realistic models of the track and ground. In particular, the layered structure of the ground should be taken into account using suitable parameter values to represent low-amplitude high-frequency vibrations [1]. For high-speed trains, it is of interest to examine the effect on the transmitted vibration as the speed of movement of a dynamic axle load approaches the speeds of waves propagating in the track and the ground.

A theoretical model for the propagation of vibration from a railway track through a ground consisting of a number of parallel layers of homogeneous material has been developed [2]. A diagram of the model is shown in Figure 1. The ground is modelled as a number of homogeneous elastic layers overlying an elastic half-space. The railway structure is represented as an infinite, continuous layered beam comprising rail, rail pad, sleepers and ballast. Only vertical dynamics of the track are considered and the two-dimensional model of the track is coupled to

*Visitor to ISVR from Department of Civil Engineering, East China Jiaotong University, Nanchang, Jiangxi 330013, People's Republic of China

0022-460X/00/130739 + 13 $35.00/0 

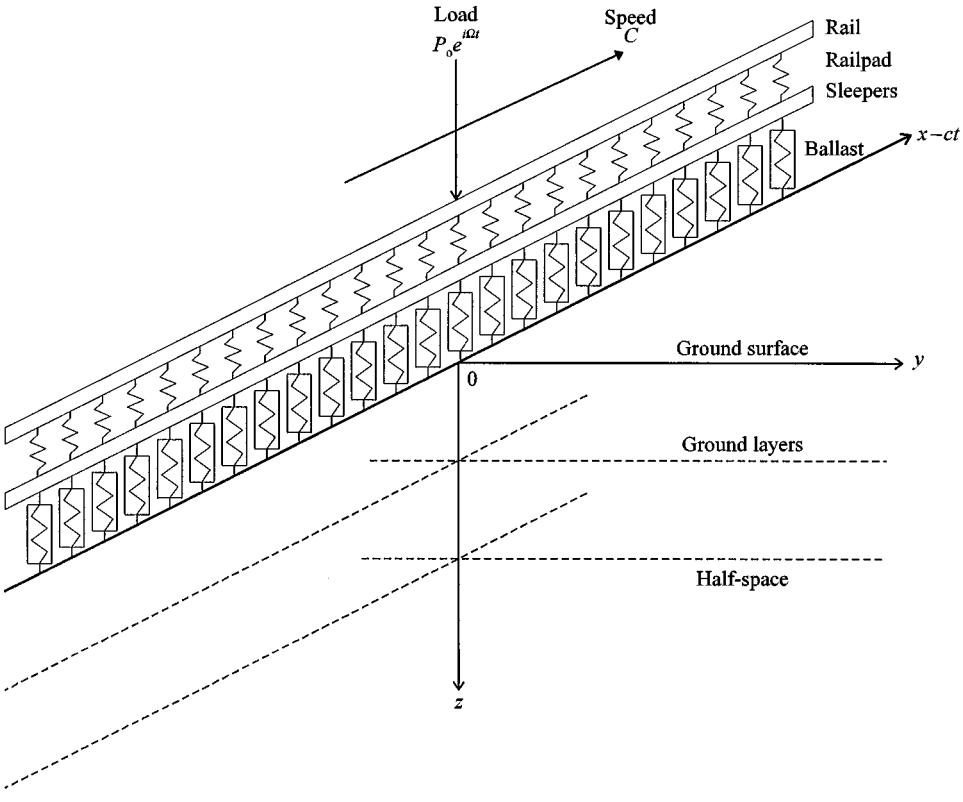


Figure 1. Diagram of the track and layered ground mode.

the ground by assuming that at each point along the track, it applies a vertical amplitude of pressure to the ground which is constant over a finite width of the ground surface. Different models for the track can be used to account for different track structure type including the effects of an embankment.

The model is described briefly here; a full description of the theory is given in reference [2]. The elastodynamic behaviour of the ground is described by Navier's equations,

$$(\lambda + \mu)\frac{\partial \Delta}{\partial x} + \mu \nabla^2 u = \rho \frac{\partial^2 u}{\partial t^2}$$

$$(\lambda + \mu)\frac{\partial \Delta}{\partial y} + \mu \nabla^2 v = \rho \frac{\partial^2 v}{\partial t^2}$$

$$(\lambda + \mu)\frac{\partial \Delta}{\partial z} + \mu \nabla^2 w = \rho \frac{\partial^2 w}{\partial t^2}$$

where $u$, $v$, $w$ are the $x$, $y$, $z$ components of displacement $\underline{u}$, $\Delta = \partial u/\partial x + \partial v/\partial y + \partial w/\partial z$ and

$$\lambda = \frac{\sigma E(1 + i\eta \operatorname{sgn}(\omega))}{(1 + \sigma)(1 - 2\sigma)}, \quad \mu = \frac{E(1 + i\eta \operatorname{sgn}(\omega))}{2(1 + \sigma)},$$

$\omega$ is the circular frequency, $E$ is the Young's modulus, $\sigma$ is the Poisson ratio and $\eta$ is the loss factor representing the material damping of the soil.

For a layered ground, a dynamic flexibility matrix $\bar{\delta}$ is obtained using the approach of Haskell and Thomson [3, 4]. This relates the response, $\underline{\bar{u}}$, of the ground surface, defined in terms of the wave number $\beta$, in the $x$ direction and $\gamma$ in the $y$ direction, to the applied forces $\underline{\bar{p}}$, i.e.,

$$\begin{Bmatrix} \bar{u}(\beta, \gamma, \omega) \\ \bar{v}(\beta, \gamma, \omega) \\ \bar{w}(\beta, \gamma, \omega) \end{Bmatrix} = [\bar{\delta}(\beta, \gamma, \omega)] \begin{Bmatrix} \bar{p}_x(\beta, \gamma, \omega) \\ \bar{p}_y(\beta, \gamma, \omega) \\ \bar{p}_z(\beta, \gamma, \omega) \end{Bmatrix}.$$

The ground is coupled via $\underline{\bar{p}}$ with a model describing the track behaviour also expressed in terms of $\beta$. The response of the ground, as a function of Cartesian co-ordinates, $\underline{u}(x, y)$ is obtained using a two-dimensional reverse Fourier transform, i.e.,

$$\underline{u}(x, y) = \frac{1}{4\pi^2} \int_{-\infty}^{\infty} \int_{-\infty}^{\infty} \underline{\bar{u}}(\beta, \gamma) e^{i(\beta x + \gamma y)} \, d\beta \, d\gamma.$$

The effect of a moving load is incorporated by adopting a co-ordinate system in the moving frame of reference and solving at the load frequency, $\Omega$, i.e., expressed in the time domain,

$$\underline{u}(x, y, z, t) = \underline{u}^*(x - ct, y, z) e^{i\Omega t},$$

where $c$ is the velocity of the load in the $x$ direction and $t$ is time.

Now, in the wave number domain, the quantity $\omega = \Omega - \beta c$ defines the equivalent frequency for the track/ground system at which the solution is carried out before the reverse Fourier transform is applied.

The model is used to predict the response of the ground surface to a vertical, unit-amplitude, oscillating force moving along the track. The steady state ground response in the moving-load frame of reference is calculated at $2048 \times 2048$ points in the wave number domain using flexibility matrices to represent the layers and the half-space. The response is then transformed into Cartesian co-ordinates using a two-dimensional FFT. In order to avoid aliasing effects, the area plotted corresponds to $512 \times 512$ points of the transform.

In order to understand the nature of vibration generation by a moving load, results from the model have been animated to show wave fronts propagating

outwards from the track in a view which moves with the load. Still pictures from the animated sequence have been reproduced in this paper. Although the lateral and longitudinal components of displacement are calculated by the model, for the purpose of the present visualization, the view presented shows the vertical component of displacement only. This is plotted for an area of ground surface extending 50 m in front of (positive direction) and behind the load and 50 m to each side of the track. The load moves along the track at a constant speed ("*train speed*") and has a frequency, $\Omega$, in its own frame of reference. Rather than plotting the amplitude of the response, the results have been plotted for an instant in time, where the load is at $0^\circ$ phase of its cycle, i.e., applying downwards. By this means the wave fronts are visible, in the still pictures, radiating outwards from the loading point.

The results are shown for three different types of ground, as described in section 2, at a number of different trains speeds and at frequencies of 10, 16 and 40 Hz. Despite the range of these parameters, for the sake of comparability, all the results are plotted to the same linear scale of displacement.

## 2. MODEL PARAMETERS

The three ground types considered are each modelled as a single layer of weathered soil overlying a half-space. It has been shown by comparison of measured and predicted response functions from a small circular source [2] that such a model of the ground is valid in the frequency range required. The properties of the three ground types for which results are shown are given in Tables 1–3.

TABLE 1

*The parameters for ground* 1

| Layer | Depth (m) | Young's modulus ($10^6$ N/m$^2$) | The Poisson ratio | Density (kg/m$^3$) | Loss factor | P-wave speed (m/s) | S-wave speed (m/s) | Rayleigh wave speed (m/s) |
|---|---|---|---|---|---|---|---|---|
| 1 | 2·0 | 269 | 0·257 | 1550 | 0·1 | 459·43 | 262·74 | 242·01 |
| Half | Space | 2040 | 0·179 | 2450 | 0·1 | 3007·4 | 1880·3 | 1707·2 |

TABLE 2

*The parameters for ground* 2

| Layer | Depth (m) | Young's modulus ($10^6$ N/m$^2$) | The Poisson ratio | Density (kg/m$^3$) | Loss factor | P-wave speed (m/s) | S-wave speed (m/s) | Rayleigh wave speed (m/s) |
|---|---|---|---|---|---|---|---|---|
| 1 | 2·0 | 60 | 0·44 | 1500 | 0·1 | 360 | 117·9 | 112 |
| Half | Space | 360 | 0·49 | 2000 | 0·1 | 1755 | 245 | 233 |

TABLE 3

*The parameters for ground 3*

| Layer | Depth (m) | Young's modulus ($10^6$ N/m$^2$) | The Poisson ratio | Density (kg/m$^3$) | Loss factor | P-wave speed (m/s) | S-wave speed (m/s) | Rayleigh wave speed (m/s) |
|---|---|---|---|---|---|---|---|---|
| 1 | 2·0 | 30 | 0·47 | 1550 | 0·1 | 340 | 81·1 | 77 |
| Half | Space | 360 | 0·49 | 2000 | 0·1 | 1755 | 245 | 233 |

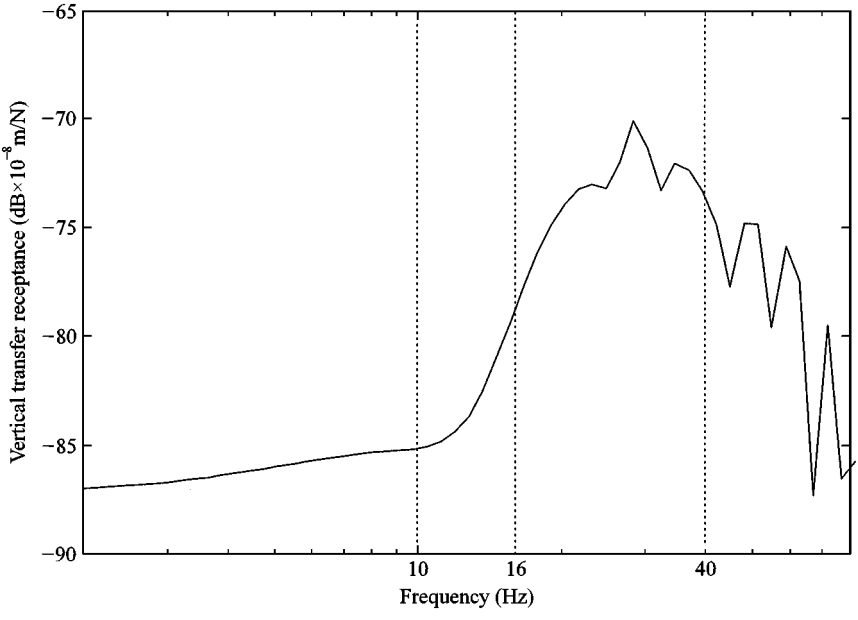


Figure 2. Vertical transfer response for ground 2 from a small circular footing to a point at 15 m distance on the ground surface.

Ground 1 represents a stiff ground consisting of a 2 m layer of weathered sandstone overlying sandstone. Ground 2 represents a clay soil, again with a 2 m weathered layer and ground 3 represents a softer weathered layer on the same substratum.

Most of the results presented are based on ground 2. Figure 2 shows the calculated vertical transfer receptance on ground 2 at 15 m from a vertical load applied via a small (0·1 m radius) circular footing. This illustrates the significance of the different frequencies shown in the subsequently presented results. At 10 Hz there is no propagating mode of vibration in the upper layer of soil via which vibration may propagate. Consequently, the response level is a function of the stiffness of the half-space substratum. The rise in the transfer receptance spectrum centred on 16 Hz corresponds to the onset of propagation in the upper layer. At 40 Hz, propagation may take place in the layer via a number of mode shapes which

TABLE 4

*The parameters for the railway track*

| | |
|---|---|
| Mass of rail beam per unit length of track | 120 kg/m |
| Bending stiffness of rail beam | $1{\cdot}26 \times 10^7$ N/m$^2$ |
| Rail pad stiffness | $3{\cdot}5 \times 10^8$ N/m$^2$ |
| Rail pad loss factor | 0·15 |
| Mass of sleepers per unit length of track | 490 kg/m |
| Mass of ballast per unit length of track | 1200 kg/m |
| Ballast stiffness per unit length of track | $3{\cdot}15 \times 10^8$ N/m$^2$ |
| Loss factor of ballast | 1·0 |
| Contact width of railway and ground | 2·7 m |

TABLE 5

*The parameters for the embankment*

| | |
|---|---|
| Mass per unit length of track | 11 000 kg/m |
| Density | 1500 kg/m$^3$ |
| Young's modulus | $60 \times 10^6$ N/m$^2$ |
| Loss factor | 0·1 |
| The Poissin ratio | 0·4 |
| Contact width of embankment and ground | 5 m |

involve coupled P-wave and vertically polarized S-wave motion ("P–SV waves" sometimes referred to as higher order Rayleigh waves [5]). The uncoupled horizontally polarized S-wave modes ("SH" or "Love" waves) are not relevant in the results presented because they contain no vertical component of motion. The slowest P–SV wave speed in the layer, at this frequency, approximates to that of the Rayleigh wave speed in a half-space of the layer material.

The parameters of the track structure for which results are presented are given in Table 4. These parameters, which are for both rails, represent a typical mainline track. Table 5 shows the parameters of the embankment which is added to the track structure for the last result presented.

## 3. THE RESULTS

The speed of wave propagation in the upper ground layer in relation to the speed of movement of the load is of primary interest in the results presented. For simplicity, the ground wave propagation speed is indicated in the Figure captions approximately by reference to the shear wave speed in the upper layer, $C_{S1}$, only. The wave speed of the first P–SV mode in the layer, which approximates to the Rayleigh wave speed of the layer material at high frequency, would be approximately 10% lower than $C_{S1}$. For simple cases of vertical loading this wave

is expected to carry most of the energy and therefore to be the most clearly visible in amplitude in the visualization. To summarize, the Figures that follow are described, therefore, by the shear wave speed in the upper layer, the frequency of oscillation of the load and the "train speed".

### 3.1. RESULTS AT GROUND 2 FOR A TRAIN SPEED BELOW THE GROUND WAVE SPEEDS

The presentation first examines the response at three different frequencies to a load moving well below the wave speed in the ground layer for the medium stiffness, ground 2. The train speed is 40 m/s (144 km/h).

Figure 3 shows the response to a 10 Hz excitation (train speed = 40 m/s, $C_{S1} = 120$ m/s (ground 2)). Near circular wave fronts can be seen propagating away from the source. The effect of the bending stiffness of the track can be seen in the deformation pattern near the load. This is asymmetric due to the motion of the load.

Figure 4 shows the response to 16 Hz excitation (train speed = 40 m/s, $C_{S1} = 120$ m/s (ground 2)). The amplitude of the waves is greater than at 10 Hz. This is consistent with the rise in transfer receptance at 16 Hz shown in Figure 2. Propagation along the track is now visible. The effect of the wave speed in the track (slower than the wave in the surrounding ground and therefore of shorter wavelength) can be seen to produce a peak in vibration amplitude running just in front of the load.

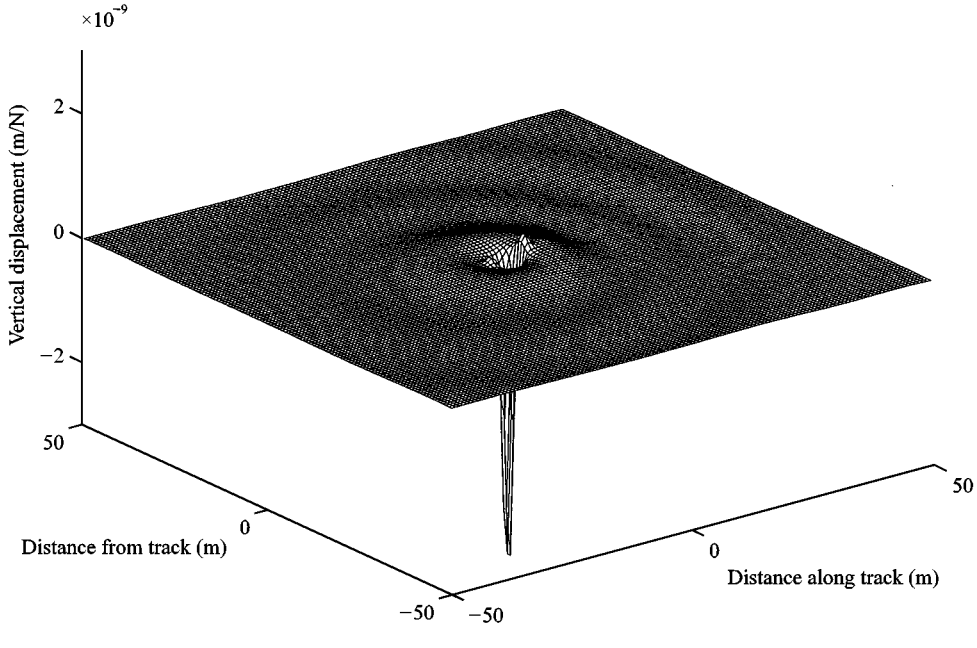


Figure 3. Vertical response of the ground surface of ground 2 ($C_S = 120$ m/s) to a unit amplitude load at 10 Hz moving at a "train speed" of 40 m/s along the track.

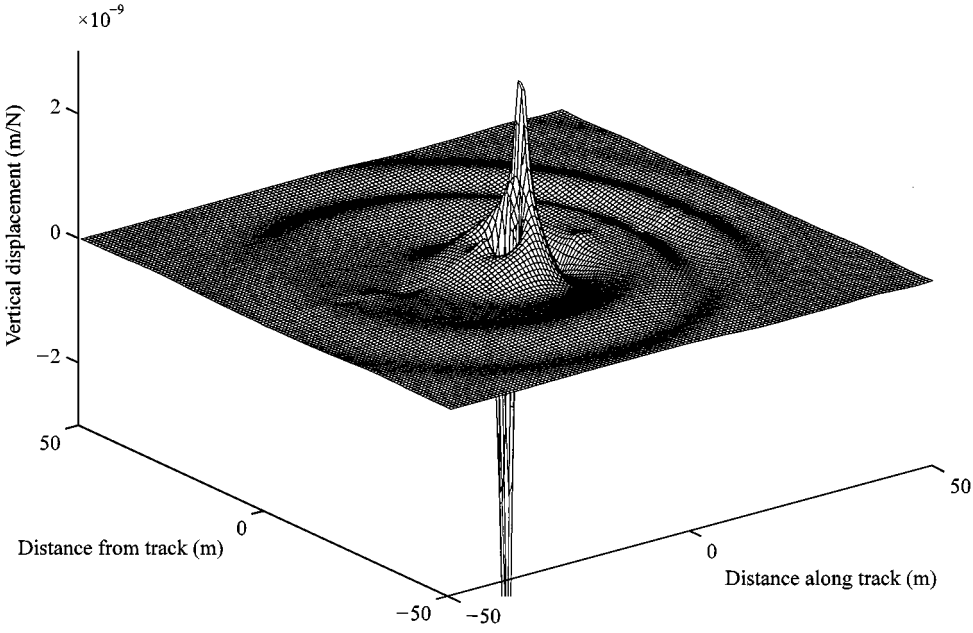


Figure 4. Frequency = 16 Hz, train speed = 40 m/s, $C_{S1}$ = 120 m/s (ground 2).

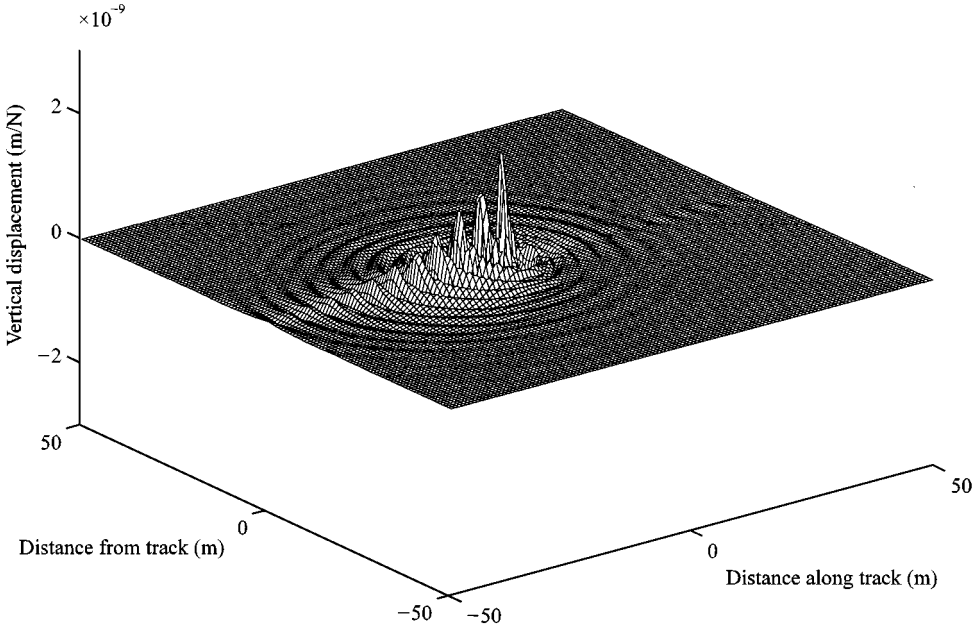


Figure 5. Frequency = 40 Hz, train speed = 40 m/s, $C_{S1}$ = 120 m/s (ground 2).

Figure 5 shows the response to a 40 Hz excitation (train speed = 40 m/s, $C_{S1}$ = 120 m/s (ground 2)). At 40 Hz the wave lengths can be seen to be much shorter than at 10 or 16 Hz due to the higher frequency of excitation and the onset

of propagation via the P–SV modes of layer. Waves propagating along the track are much stronger at this frequency and trail behind the load. The high level of vibration under the track behind the load leads to a higher amplitude in the ground near to the track here than ahead of the load.

### 3.2. EFFECT OF VARYING THE TRAIN SPEED

Figure 6 shows the response to a 40 Hz excitation at a train speed of 83 m/s ($C_{S1} = 120$ m/s (ground 2)). Keeping the frequency at 40 Hz, the train speed is now increased to 83 m/s (30 km/h). Compared with Figure 5, where circular wave propagation was shown, the waves can be seen to be of greater amplitude behind the load than in front. The waves in the track show a lower rate of attenuation with distance from the moving load. The source appears more like an extended source with interference patterns visible in the wave field.

Figure 7 shows results for a train speed of 100 m/s (frequency = 40 Hz, $C_{S1} = 120$ m/s (ground 2)). The load now moves at about the speed of the first P–SV wave in the layer. The result is that now no vibration of this mode appears propagating across the ground surface away from the track ahead of the load and an effect analogous to the bow wave of a ship can be seen. Although the speed of travel of the load is near the main wave speed of propagation in the ground, the amplitude of vibration at distances away from the track is not greatly increased compared to Figure 5 and 6.

Waves of significant amplitude under the track can be seen ahead of the load. In the animated visualization these appear to be propagating "backwards", towards

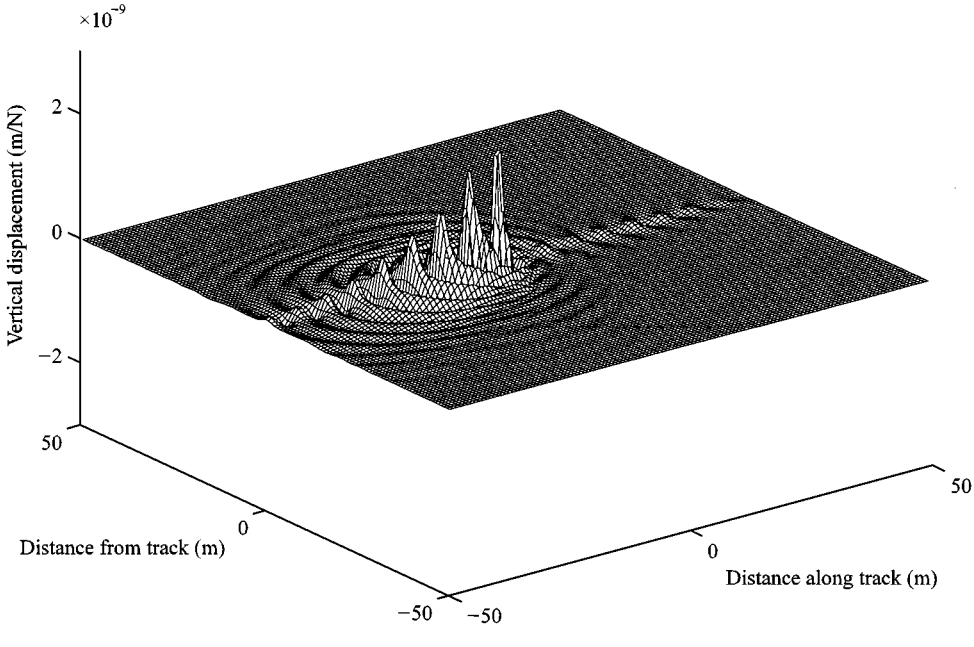


Figure 6. Frequency = 40 Hz, train speed = 83 m/s, $C_{S1} = 120$ m/s (ground 2).

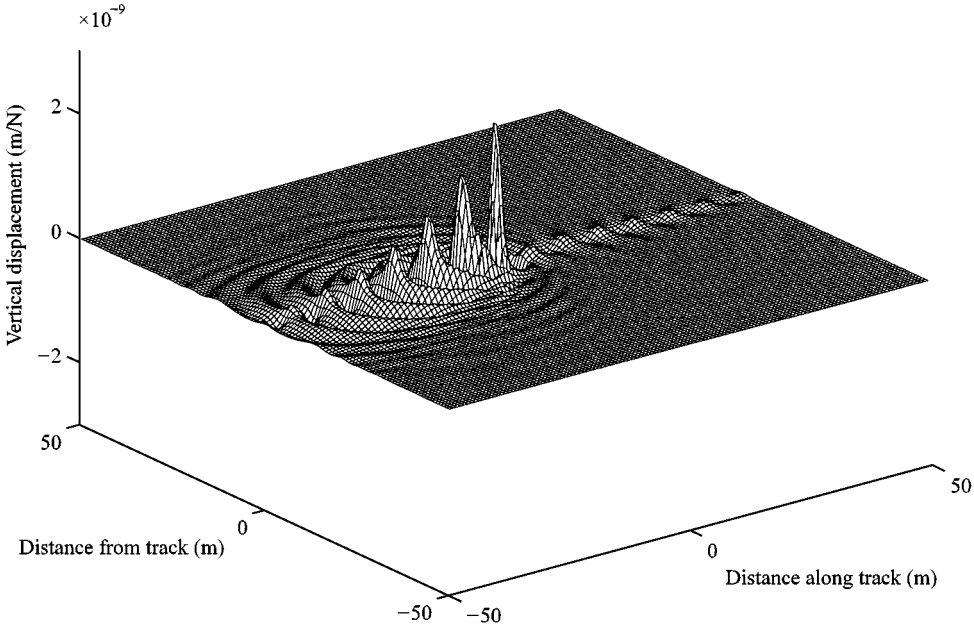


Figure 7. Frequency = 40 Hz, train speed = 110 m/s, $C_{S1}$ = 120 m/s (ground 2).

the load, as they move more slowly than the load. These waves are thought to be the result of excitation of the track by vibration propagating forwards from the load via high order mode of vibration of the track/ground which still have a wave speed well in excess of the train speed.

### 3.3. EFFECT OF GROUND TYPE

The next two cases show the effects as a load moves at a constant speed of 83 m/s (300 km/h) over grounds 1 and 3 having a shear wave speed below the train speed. Figures 8, 6 and 9, in that order, therefore form a sequence in which the train speed remains constant at 83 m/s and the ground becomes progressively softer.

Figure 8 shows the response on ground 1 ($C_{S1}$ = 260 m/s) (frequency = 40 Hz, train speed = 83 m/s). On the hard ground, the behaviour with the higher wave speed in the soil is similar to that of the softer ground at lower frequency. The wavelengths can be seen to be longer than in Figure 6 where the train speed and load frequency are the same but the ground is softer. The waves under the track have a higher wave speed than the speed of the load in this case, and so propagate ahead of it.

Figure 9 shows the response on ground 3 ($C_{S1}$ = 80 m/s) (frequency = 40 Hz, train speed = 83 m/s). On the softer ground, the Rayleigh wave speed is now lower than that of the load. A strong component of a higher order mode of vibration is seen. This has a higher wave speed than the train speed (long wavelength, circular wave fronts). The shorter wavelength wave is still present and is restricted to

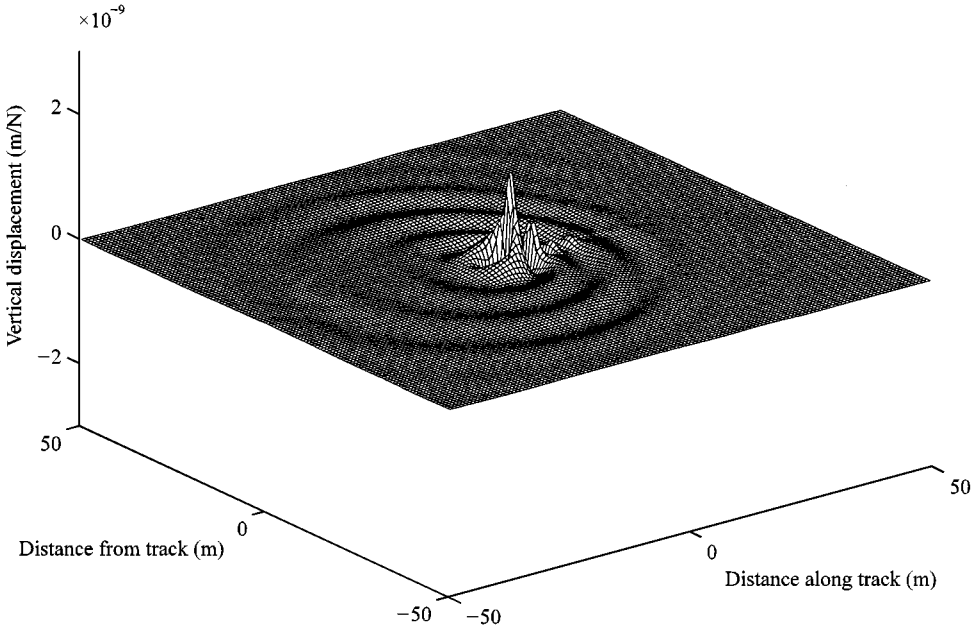


Figure 8. Frequency = 40 Hz, train speed = 83 m/s, $C_{S1}$ = 260 m/s (ground 1).

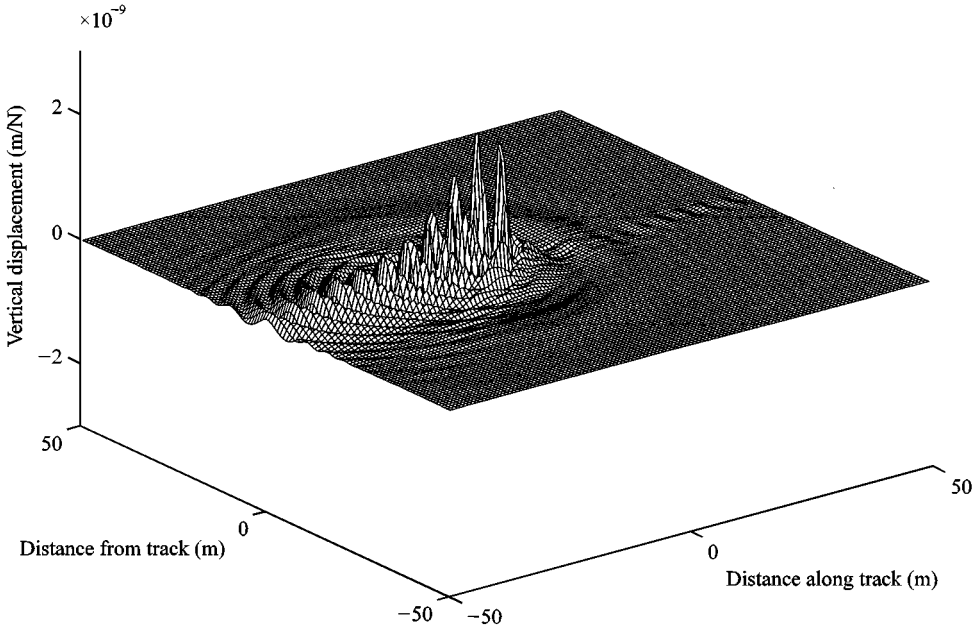


Figure 9. Frequency = 40 Hz, train speed = 83 m/s, $C_{S1}$ = 80 m/s (ground 3).

a shallow angle behind the load with higher amplitude of propagation at certain angles. The track vibration has a low rate of decay with distance behind the load.

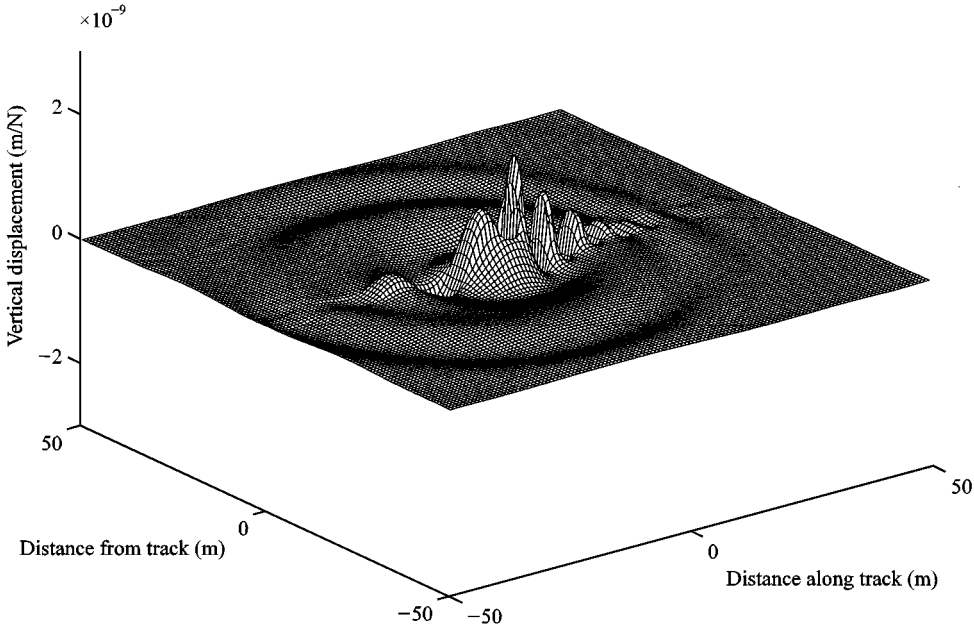


Figure 10. Frequency = 16 Hz, train speed = 40 m/s, $C_{S1}$ = 120 m/s (ground 2), with embankment.

### 3.4. EFFECT OF EMBANKMENT

Figure 10 shows the effects at 16 Hz of a change in the track. Here a 1 m high embankment has been added below the track structure. The result is shown on ground 2 and at a train speed of 40 m/s and so is comparable to Figure 4 with the previous track model. From the vibration field, the width of the embankment under the track can be seen to be greater than that of previous examples (now 5 m rather than 2·7 m). The effect of the stiffer and more massive track structure (i.e., including the embankment) results in a lower level of vibration at the loading point but higher amplitudes being spread along the track. This causes significant changes in vibration amplitude near the track. However, the level of vibration propagating to the far field is not greatly affected.

## 4. CONCLUSIONS

The results presented have shown that for loads travelling at high speeds, comparable to the speeds of vibration propagation in the track/ground structure, a number of effects are to be expected. High levels of vibration may be expected to occur in the ground under, or very near to, the track. These may manifest themselves ahead of, or in the wake of the load. For frequencies of excitation where a number of P–SV modes exist, no large increase in propagated vibration amplitude occurs as the train speed approaches and exceeds the phase velocities of the first PS–V mode. In this case, the vibrational energy transfers to a higher order mode.

## ACKNOWLEDGMENT

C. J. C. Jones wishes to acknowledge the financial support of the EPSRC under research grant GR/L11397 for his participation in this work.

## REFERENCES

1. C. J. C. Jones 1994 *Proceedings of the Institution of Civil Engineers, Transportation* **105**, 43–51. Use of numerical models to determine the effectiveness of anti-vibration systems for railways.
2. X. Sheng, C. J. C. Jones and M. Petyt 1999 *Journal of Sound and Vibration* **228**, 129–156. Ground vibration generated by a load moving along a railway track.
3. N. Haskell 1953 *Bulletin of the Seismological Society of America* **73**, 17–43. The dispersion of surface waves on multilayered media.
4. W. T. Thomson 1950 *Journal of Applied Physics* **21**, 81–93. Transmission of elastic waves through a stratified soil medium.
5. F. S. Grant and G. F. West 1965 *McGraw Hill International Series in the Earth Sciences.* Interpretation theory in applied geophysics.